Springer

Dear Author,

Here are the proofs of your article.

- You can submit your corrections **online**, via **e-mail** or by **fax**.
- For **online** submission please insert your corrections in the online correction form. Always indicate the line number to which the correction refers.
- You can also insert your corrections in the proof PDF and **email** the annotated PDF.
- For fax submission, please ensure that your corrections are clearly legible. Use a fine black pen and write the correction in the margin, not too close to the edge of the page.
- Remember to note the **journal title**, **article number**, and **your name** when sending your response via e-mail or fax.
- **Check** the metadata sheet to make sure that the header information, especially author names and the corresponding affiliations are correctly shown.
- **Check** the questions that may have arisen during copy editing and insert your answers/ corrections.
- **Check** that the text is complete and that all figures, tables and their legends are included. Also check the accuracy of special characters, equations, and electronic supplementary material if applicable. If necessary refer to the *Edited manuscript*.
- The publication of inaccurate data such as dosages and units can have serious consequences. Please take particular care that all such details are correct.
- Please **do not** make changes that involve only matters of style. We have generally introduced forms that follow the journal's style.
  Substantial changes in content, e.g., new results, corrected values, title and authorship are not allowed without the approval of the responsible editor. In such a case, please contact the Editorial Office and return his/her consent together with the proof.
- If we do not receive your corrections **within 48 hours**, we will send you a reminder.
- Your article will be published **Online First** approximately one week after receipt of your corrected proofs. This is the **official first publication** citable with the DOI. **Further changes are, therefore, not possible.**
- The **printed version** will follow in a forthcoming issue.

Please note

After online publication, subscribers (personal/institutional) to this journal will have access to the complete article via the DOI using the URL: http://dx.doi.org/[DOI].
If you would like to know when your article has been published online, take advantage of our free alert service. For registration and further information go to: http://www.link.springer.com.

Due to the electronic nature of the procedure, the manuscript and the original figures will only be returned to you on special request. When you return your corrections, please inform us if you would like to have these documents returned.

Metadata of the article that will be visualized in OnlineFirst

Please note: Images will appear in color online but will be printed in black and white.

ArticleTitle	Powder Removal from Ti-6Al-4V Cellular Structures Fabricated via Electron Beam Melting	
Article Sub-Title		
Article CopyRight	The Minerals, Metals & Materials Society (This will be the copyright line in the final PDF)	
Journal Name	JOM	
Corresponding Author	Family Name	**Harrysson**
	Particle	
	Given Name	**Ola L.A.**
	Suffix	
	Division	Edward P. Fitts Department of Industrial and Systems Engineering
	Organization	NC State University
	Address	Raleigh, NC, USA
	Email	harrysson@ncsu.edu
Author	Family Name	**Hasib**
	Particle	
	Given Name	**Hazman**
	Suffix	
	Division	Manufacturing Design Department
	Organization	University Teknikal Malaysia Melaka
	Address	Durian Tunggal, Malaysia
	Email	
Author	Family Name	**West**
	Particle	
	Given Name	**Harvey A.**
	Suffix	II
	Division	Edward P. Fitts Department of Industrial and Systems Engineering
	Organization	NC State University
	Address	Raleigh, NC, USA
	Email	

Schedule	Received	5 January 2015
	Revised	
	Accepted	16 January 2015

Abstract

Direct metal fabrication systems like electron beam melting (EBM) and direct metal laser sintering (also called selective laser melting) are gaining popularity. One reason is the design and fabrication freedom that these technologies offer over traditional processes. One specific feature that is of interest is mesh or lattice structures that can be produced using these powder-bed systems. One issue with the EBM process is that the powder trapped within the structure during the fabrication process is sintered and can be hard to remove as the mesh density increases. This is usually not an issue for the laser-based systems since most of them work at a low temperature and the sintering of the powder is less of an issue. Within the scope of this project, a chemical etching process was evaluated for sintered powder removal using three different cellular structures with varying mesh densities. All meshes were fabricated via EBM using Ti6Al4V

powder. The results are promising, but the larger the structures, the more difficult it is to completely remove the sintered powder without affecting the integrity of the mesh structure.

Footnote Information

JOM
DOI: 10.1007/s11837-015-1307-x

Powder Removal from Ti-6Al-4V Cellular Structures Fabricated via Electron Beam Melting

HAZMAN HASIB,[1] OLA L.A. HARRYSSON,[2,3] and HARVEY A. WEST II[2]

1.—Manufacturing Design Department, University Teknikal Malaysia Melaka, Durian Tunggal, Malaysia. 2.—Edward P. Fitts Department of Industrial and Systems Engineering, NC State University, Raleigh, NC, USA. 3.—e-mail: harrysson@ncsu.edu

Direct metal fabrication systems like electron beam melting (EBM) and direct metal laser sintering (also called selective laser melting) are gaining popularity. One reason is the design and fabrication freedom that these technologies offer over traditional processes. One specific feature that is of interest is mesh or lattice structures that can be produced using these powder-bed systems. One issue with the EBM process is that the powder trapped within the structure during the fabrication process is sintered and can be hard to remove as the mesh density increases. This is usually not an issue for the laser-based systems since most of them work at a low temperature and the sintering of the powder is less of an issue. Within the scope of this project, a chemical etching process was evaluated for sintered powder removal using three different cellular structures with varying mesh densities. All meshes were fabricated via EBM using Ti6Al4V powder. The results are promising, but the larger the structures, the more difficult it is to completely remove the sintered powder without affecting the integrity of the mesh structure.

INTRODUCTION

Cellular metals, also known as metal foams, can be explained as solid metals exhibiting cellular structures that form voids called pores. In general, there are two broad categories of metal foams, stochastic and nonstochastic geometries. Briefly, stochastic foams have random variations in the shape and size of the cells, whereas in contrast, periodic cellular structures have repeating lattice structures and can be categorized by their shapes and sizes.

Cellular structures can be used for numerous purposes such as filters, silencers, supports for catalysts, and heat exchangers.[1] Another area of use for these structures is biomedical implants where tissue ingrowth is needed. According to Harrysson et al.,[2] the fixation strength of a cementless implant relies on its pore size. Tissues need certain surface conditions to grow on, and the same research has summarized that pore sizes between 50 μm and 800 μm are usually found to fulfill the requirements for bone tissue.

This research addresses the problem by studying different cellular structures made by the electron beam melting (EBM) process with customized pore sizes and looks at methods for removing the trapped powder. Chua et al.[3] indicated that this is a common problem for powder-based additive manufacturing (AM) processes, especially when a large part is made and the trapped powder is beyond reach. A research project on Ti-6Al-4V for biomedical applications by Li et al.[4] found that cellular structures fabricated by EBM are covered with loosely sintered metal particles and suggested that some cleaning process needs to be used to remove them.

The purpose of this research is to fabricate different nonstochastic Ti-6Al-4V cellular structures with pore sizes below 800 μm and to investigate the feasibility and effectiveness of cleaning the trapped powder inside the structures with a chemical etching technique using hydrofluoric-nitric acid solutions at different etching periods. Three different cell geometries were used to build the samples: hexagon, octahedron, and rhombic dodecahedron.

Our hypothesis is that the chemical etching will decrease the diameter of the struts leading to an increased porosity while dissolving the trapped sintered powder inside the mesh structure. Because the trapped powder particles have a much larger surface area then the solid struts, we hypothesize

that the trapped powder will dissolve much faster than the solid struts leading to a clean mesh structure. The ideal initial structure should have struts that are oversized, leading to a high initial density with "small" pores. After the etching, the trapped powder should be dissolved and the resulting mesh structure should have the desired density and pore sizes. Furthermore, the chemical etching will lead to smoother struts that will increase the overall fatigue life of the structure.

ELECTRON BEAM MELTING

The EBM process is a powder-bed-based direct metal fabrication process that uses a high power electron beam (4.5 kW) to selectively melt thin layers of metal powder (50 μm) in successive layers. The process is taking place under vacuum at an elevated temperature. The temperature is dependent on the material, and for Ti6Al4V, a base temperature of 750°C is used.[5] The vacuum level is controlled to approximately 2×10^{-3} bar to keep the beam focus constant. To maintain the elevated temperature, the electron beam is used to preheat each fresh layer of powder before melting takes place. The beam is scanned over the entire build area at a high speed and low power. The preheating serves two purposes when processing metals with low electrical conductivity. First, the elevated temperature of the powder is maintained, and second, the powder is lightly sintered together to increase the bulk electrical conductivity to prevent the powder particles from charging and repelling each other. This phenomenon is referred to as "smoke" by Arcam AB (Mölndal, Sweden) and happens when the electrons are not dissipated to ground fast enough due to low conductivity. While the sintering of the powder helps the process, it makes it more difficult to remove "loose" powder from internal features. This is particularly important when fabricating mesh structures. Because of the elevated temperature throughout the build, the final parts have very low internal residual stresses and usually do not need post heat treatment. Standard process parameters developed by Arcam were used for these builds.

STRUCTURAL CHARACTERISTICS

Relative Density

Gibson and Ashby[6] indicated that relative density is the most important structural feature for metallic foams. In general, relative density is the ratio of the foam's density to the density of the solid material that the foam is made of, calculated by ρ/ρ_s (where ρ is the density of the foam and ρ_s is the density of the solid). The porosity of a cellular structure is simply $(1 - \rho/\rho_s)$ and can be defined as the volume fraction occupied by the pore space in the structure. Ashby[7] and Wadley[8] suggested that the relative density in a structure can be manipulated by modifying the cell's edge length and wall thickness. Both references provided mathematical equations on calculating relative density for certain cell geometries in relation to their edge length and wall thickness.

Cell Topology and Shape

Cell topology can be either closed cells or open cells. Closed cells have membrane-like surfaces that seal them off from the neighboring cells.[6] For bone ingrowth purposes, the cell structure must be open. Besides topology, cell shape also plays an important role in contributing to the structure's properties. In three-dimensional arrays, various cell shapes can be packed together to fill the space and build up a nonstochastic cellular structure. Figure 1 shows several shapes of unit cells, and Table I summarizes the properties of unit cell geometries commonly considered for cellular structures (where h is the

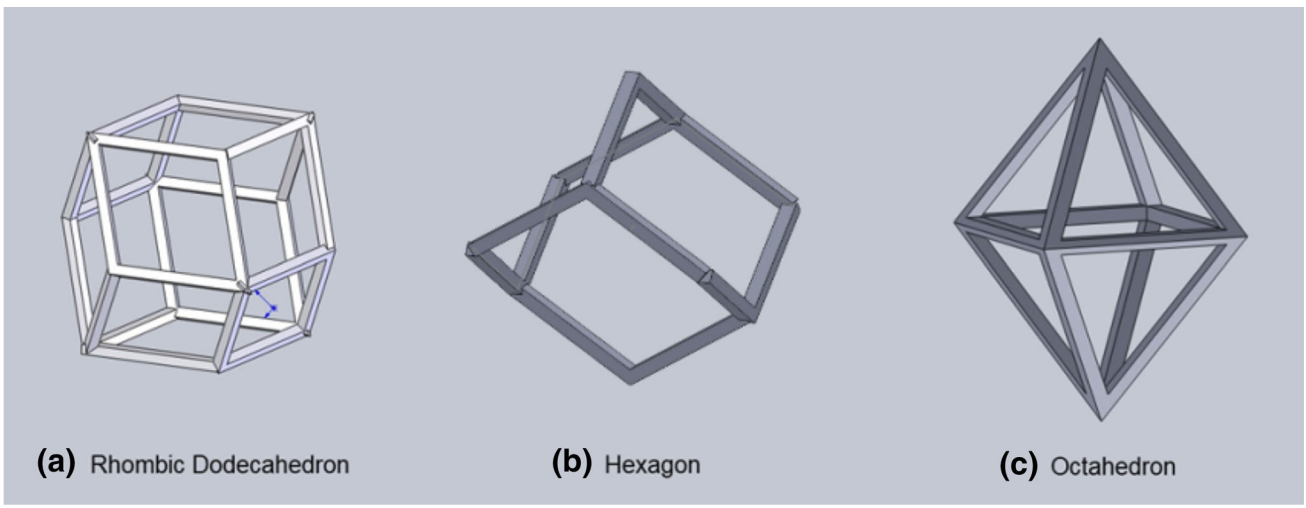

Fig. 1. Examples of commonly used unit cells.

Journal : 11837_JOM | Dispatch : 31-1-2015 | Pages : 8
Article No.: 1307 | ☐ LE ☑ CP | ☐ TYPESET ☑ DISK

Table I. Geometric property of unit cells[6]

Cell shape	Cell volume	Surface area	Edge length
Tetrahedron	$0.118l^3$	$3l^2$	$6l$
Triangular prism	$0.433lh^2$	$0.86l^2 + 3lh$	$6l + 3h$
Square prism	lh^2	$2l^2 + 4lh$	$8l + 4h$
Hexagonal prism	$2.598lh^2$	$3l^2 + 6lh$	$12l + 6h$
Octahedron	$0.471l^3$	$3.46l^2$	$12l$
Rhombic dodecahedron	$2.79l^3$	$10.58l^2$	$24l$

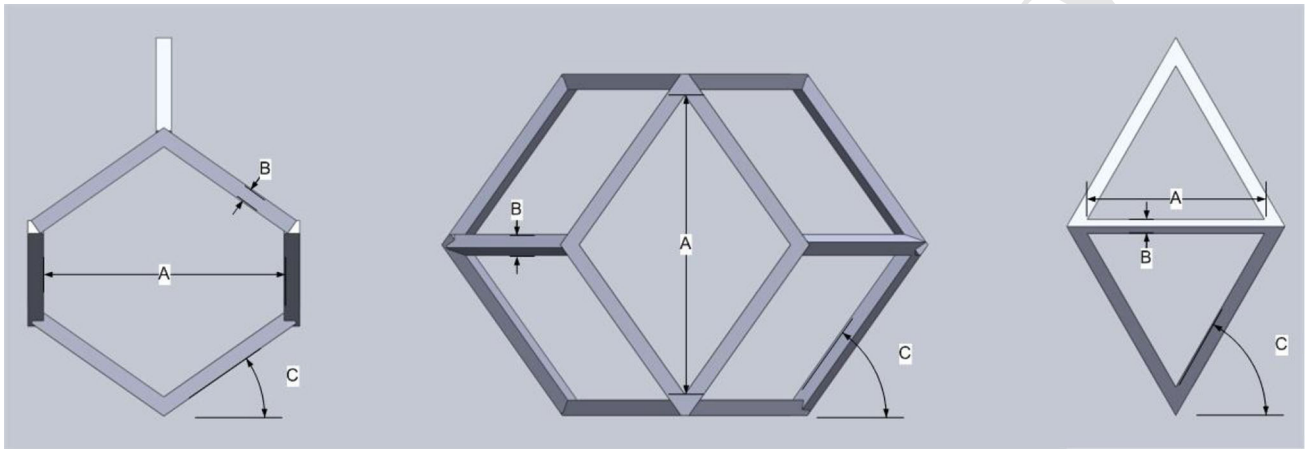

Fig. 2. Unit cell characteristics for hexagonal, rhombic dodecahedral, and octahedral: (a) is the pore size, (b) is the strut size, and (c) is the build angle.

height of the unit cell and l is the length of the strut).

Design and Fabrication of Structures

Three different polyhedral structures were selected as the unit cells for the described research: hexagonal, rhombic dodecahedral, and octahedral cell structures. Their unit cells were designed in SolidWorks (Dassault Systèmes SolidWorks Corp., Waltham, MA) with the characteristics shown in Fig. 2. These unit cells were patterned to fill space and form a cube with the dimensions of approximately 25.4 mm × 25.4 mm × 25.4 mm. The struts were designed with a square cross section rather than a circular one to reduce the size of the stereolithography (STL) files. During the melting of these thin struts, the resulting cross section will be more circular than square. Because of SolidWorks' limitations, most of the patterning procedures were carried out using Magics software (Materialise, Leuven, Belgium). After the unit cells were completely patterned, the STL files were checked for errors and corrected in the same software before being exported them to the EBM build software.

The build substrate was first preheated to 750°C by scanning the electron beam over it before the first layer of Ti6Al4V powder was deposited and melted. The successive layers were melted according to the above described process until the build was completed. The build chamber was cooled with helium gas after the completion of each build. Parts were taken out of the chamber and initially cleaned with pressurized air containing titanium powder, which is the standard method for cleaning Ti6Al4V EBM parts. To observe and compare the chemical etching effects toward removing the trapped powder in the later stage of this research, the cleaning time was set to 3 min for each cube, where each surface of the cube was blasted for 30 s.

The pore size of the structures needs to be less than 800 μm to obtain good bone tissue ingrowth. To acquire the right pore size for these structures, they were built in decreasing scales (Fig. 3), and the resulting pores were measured using a Hirox KH-7700 (Hirox-USA, Hackensack, NJ) digital microscope as shown in Fig. 4. The number of cells was kept constant so the size of the cubes decreased with decreasing unit cells. Based on this scaling method, it was found that the initial pore and strut values in Table II produced pore sizes of approximately 600 μm.

Chemical Etching Procedure

Several acids such as hydrochloric acid (HCl), sulfuric acid (H_2SO_4), hydrofluoric acid (HF), and nitric acid (HNO_3) are known to react with

titanium. However, titanium and its alloys require strong etchants to remove the adherent oxide film on their surface; thus, a combination of HF and HNO_3 is commonly found in the etchants.[9] However, proper ratios of both acids in the solution need to be selected carefully as it will affect the etching rate and the amount of hydrogen absorbed in cast Ti-6Al-4V.[10] It was found that larger amounts of HNO_3 will reduce hydrogen absorption. Brunette et al.[11] also suggested that the ratio of HF to HNO_3 needs to be at a ratio of 1:10 to reduce hydrogen absorption, which will lead to surface embrittlement.

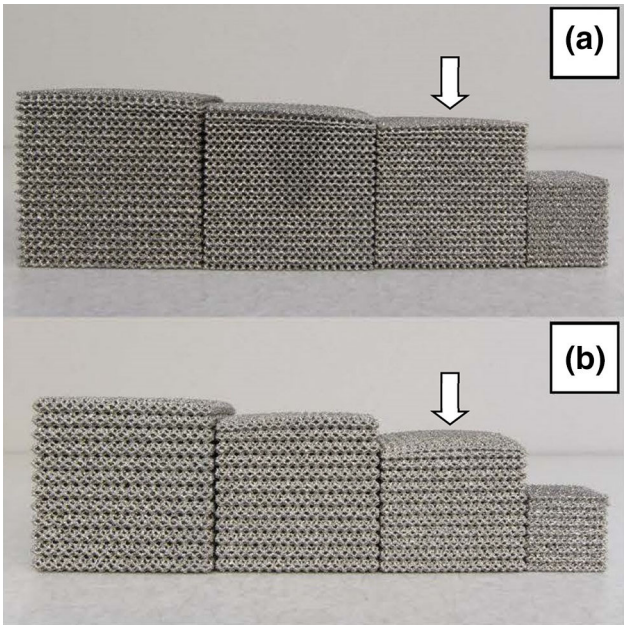

Fig. 3. Scaling of structures: (a) hexagonal mesh structures and (b) rhombic dodecahedral mesh structures. Structures used in this research are marked by the arrows in the picture.

A preliminary study was conducted to determine suitable etching conditions for this research project. Twelve Ti-6Al-4V cubic mesh specimens were fabricated via EBM (four specimens for each cell shape) and the sizes were approximately 25.4 mm × 25.4 mm × 25.4 mm. Pre-etched relative densities for the hexagonal, rhombic dodecahedral, and octahedral specimens were measured and the average values obtained were 0.33, 0.19, and 0.45, respectively. These specimens had larger pore sizes than the specimens used later in this project. Four groups consisting of three specimens, one from each cell type, were formed and etched in hydrofluoric-nitric acid solution (2% HF, 20% HNO_3, and the balance is H_2O) under four different combinations of etchant volume and etching time: 200 mL for 90 s, 200 mL for 120 s, 400 mL for 90 s, and 400 mL for 120 s. After each etching process, the samples were rinsed inside a deionized water bath six times and dried with nitrogen. Postetched relative densities were measured and compared with the pre-etched ones. The reductions in the relative densities are shown in Fig. 5.

The results show that the etchant volume affects the material removal quantity only when a longer etching time is used. The corrosive agent in the

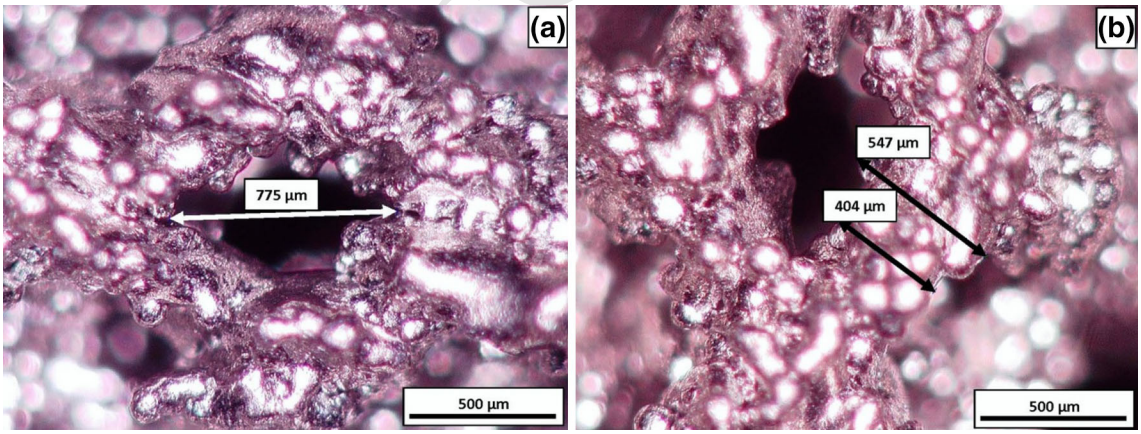

Fig. 4. Pore measurement (a) and strut measurement (b) with Hirox KH-7700 digital microscope under ×100 magnification.

Table II. Characteristics of unit cells used for the rest of the research

Unit cell shape	Initial pore size (A) (mm)	Initial strut size (B) (mm)	Strut angle (C) (°)
Hexagon	1.2	0.1	30
Rhombic dodecahedron	1.5	0.1	54.74
Octahedron	1.4	0.1	53.13

Journal : 11837_JOM Dispatch : 31-1-2015 Pages : 8
Article No.: 1307 ☐ LE ☑ CP ☐ TYPESET ☑ DISK

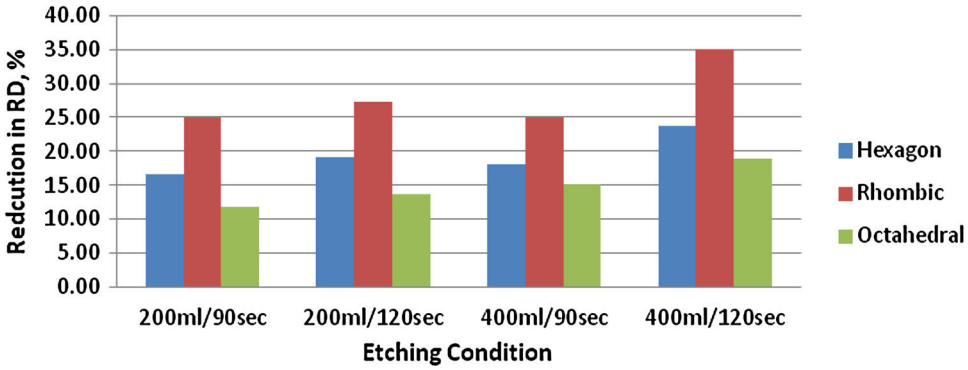

Fig. 5. Average of percentage reduction in relative density for different etching conditions.

Table III. Allocation of samples for chemical etching

	Sample size, *n*			
Unit cell shape	**Nonetched**	**90 s**	**120 s**	**Total**
Hexagon	3	3	3	27
Rhombic dodecahedron	3	3	3	
Octahedron	3	3	3	

etchant depleted over time and the etching rate decreased. This effect was expected to become greater when the actual specimens were used as they have more trapped powder due to their much smaller pore sizes. It can be seen that the first three conditions have similar results except for the octahedral. Based on this preliminary study, two etching conditions were selected for further tests: 400 mL for 90 s and 400 mL for 120 s. Table III summarizes the number of specimens made and their allocations in this research.

Estimation of Trapped Powder

Nine samples were used to evaluate the effect of chemical etching toward reducing the amount of trapped powder inside the meshes, three samples for each cell type, which consist of unetched, 90 s etching, and 120 s etching. Each cube was mounted in low-viscosity resin and placed in a vacuum chamber to ensure full penetration. The mounted specimens were parted into two sections parallel to the build direction with a water-cooled SiC abrasive cut-off saw. Next, the parting surface was polished to obtain an optimal surface for microscopic inspection. The amount of trapped powder was measured in terms of surface area as the region with and without powder inside the mesh can be differentiated distinctively. The surfaces were also inspected under a Hirox KH-7700 digital microscope. Figure 6 shows the cross-sectional area of a parted hexagonal cube.

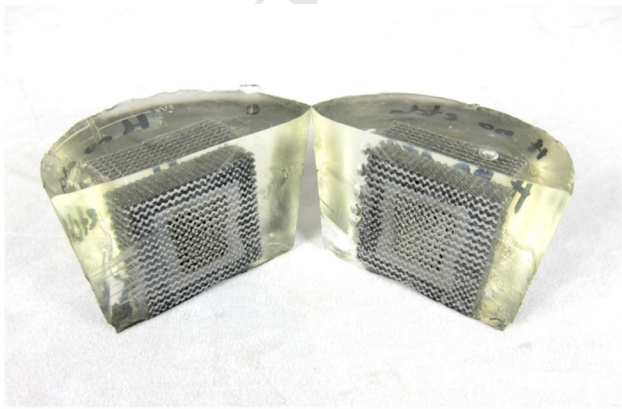

Fig. 6. Cross sections of a cube with a hexagonal structure showing the trapped powder inside.

SUMMARY OF RESULTS

Measurements of Structures

Twenty-seven parts were measured in terms of their strut and pore sizes. Twelve readings were taken from each specimen, three from each surface parallel to the build direction (four surfaces in total). The top and bottom surfaces of the cubes were not measured because they have different cell layouts. Tables IV and V list the measurement results of struts and pores respectively, measured with the Hirox KH-7700 digital microscope. The values presented are the averages of three specimens. The results show that the corrosive action from the chemical etching processes clearly reduced the mass of the structures, hence decreasing their relative densities.

Trapped Powder Removal

The amount of trapped powder within the mesh structures was measured by calculating the area possessed by the powder for each cube's cross section as shown in Fig. 7. A standard measuring ruler was used as it was not possible to obtain the entire image of the cross section with the Hirox KH-7700 digital microscope even with the lowest magnifica-

Table IV. Strut sizes of lattice structures in different etching conditions

Structure	Etching condition	Average strut diameter (μm)	Standard deviation (μm)	Average relative density
Hexagonal	Not etched	515.13	40.32	0.3583
	90 s	376.02	33.81	0.3217
	120 s	302.30	23.40	0.2807
Rhombic dodecahedral	Not etched	478.28	31.77	0.3604
	90 s	300.84	35.03	0.3105
	120 s	253.80	22.08	0.2955
Octahedral	Not etched	467.70	36.43	0.4108
	90 s	357.09	31.47	0.3425
	120 s	311.14	23.28	0.3182

Table V. Pore sizes of lattice structures in different etching conditions

Structure	Etching condition	Average pore size (μm)	Standard deviation (μm)	Average relative density
Hexagonal	Not etched	572.41	48.08	0.3583
	90 s	726.65	61.14	0.3217
	120 s	864.03	50.81	0.2807
Rhombic dodecahedral	Not etched	603.96	56.59	0.3604
	90 s	907.95	67.90	0.3105
	120 s	1057.02	73.43	0.2955
Octahedral	Not etched	601.88	57.26	0.4108
	90 s	843.31	75.85	0.3425
	120 s	951.48	59.84	0.3182

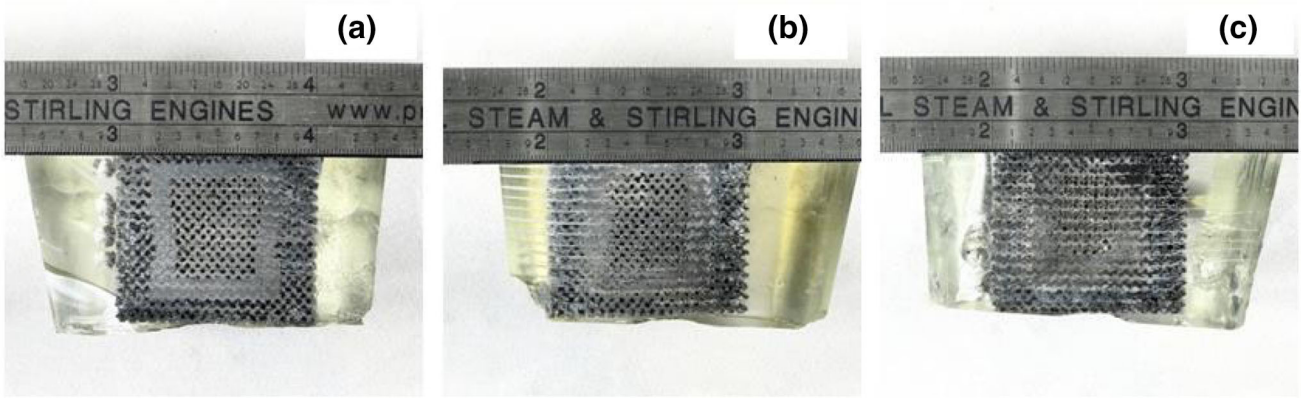

Fig. 7. Cross sections of hexagon cubes showing the trapped powder inside the mesh structures: (a) not etched, (b) 90 s etched, and (c) 120 s etched.

tion. Furthermore, the areas occupied by the powder are approximately rectangular in shape, so measuring their edges was straightforward. Table VI lists the outcomes of the evaluation, and Fig. 8 shows the microscopic observations under Hirox KH-7700 digital microscope. As can be seen from the images, the trapped sintered powder is denser in the nonetched sample than in the etched samples. Even between the 90 s sample and the 120 s sample, there is a difference in remaining sintered powder density. Furthermore, the images show that the strut cross sections are smaller in the etched samples than in the nonetched sample.

DISCUSSION AND CONCLUSION

Nonstochastic Ti-6Al-4V cellular structures with small pore sizes (approximately 600 μm) have been successfully fabricated via EBM. The scaling method has been used to tailor and determine the

initial pore sizes in the SolidWorks' drawing files to obtain the required final pore sizes. Fabrication of structures with smaller pore sizes has not been successful because of the machine's resolution at the time. When attempting to fabricate meshes with smaller pores, most of the pores are not fully opened and their shapes are not consistent. It is anticipated that smaller pore sizes will be possible to fabricate in the near future as the EBM technology continues to develop.

Table VI. Measured area of trapped powder inside the cellular structures

Unit cell	Etching condition	Area of trapped powder (mm^2)
Hexagonal	Not etched	298.06
	90 s	316.13
	120 s	297.29
Rhombic Dodecahedral	Not etched	243.87
	90 s	245.68
	120 s	260.13
Octahedral	Not etched	261.93
	90 s	270.97
	120 s	254.45

The chemical etching approach used to remove the trapped powder within the structures does not seem completely successful and conclusive. While the etched samples were reduced in weight, relative density, and strut size, little significant changes in trapped powder were observed from the samples' cross sections. Further inspection under the Hirox KH-7700 digital microscope clearly showed the region with and without powder, but there were no other indications to differentiate between the unetched and etched structures. It is not clear how much the decrease in weight was contributed by the strut sizes reduction and the trapped powder removal. The results also indicate that the hexagonal structures have the most powder trapped in every condition. This is consistent with their pore sizes which are relatively smaller compared to rhombic dodecahedral and octahedral structures. From Fig. 7, it can be seen that the cross sections seem to have a "frame" of denser powder an equal distance from the surfaces. This phenomenon was seen in all the specimens. The authors hypothesized that this is powder that is being compressed during the blasting session. Because each sample is blasted with compressed air and titanium powder from each direction for the exact same period of time, the depth is consistent. Due to the compaction of the

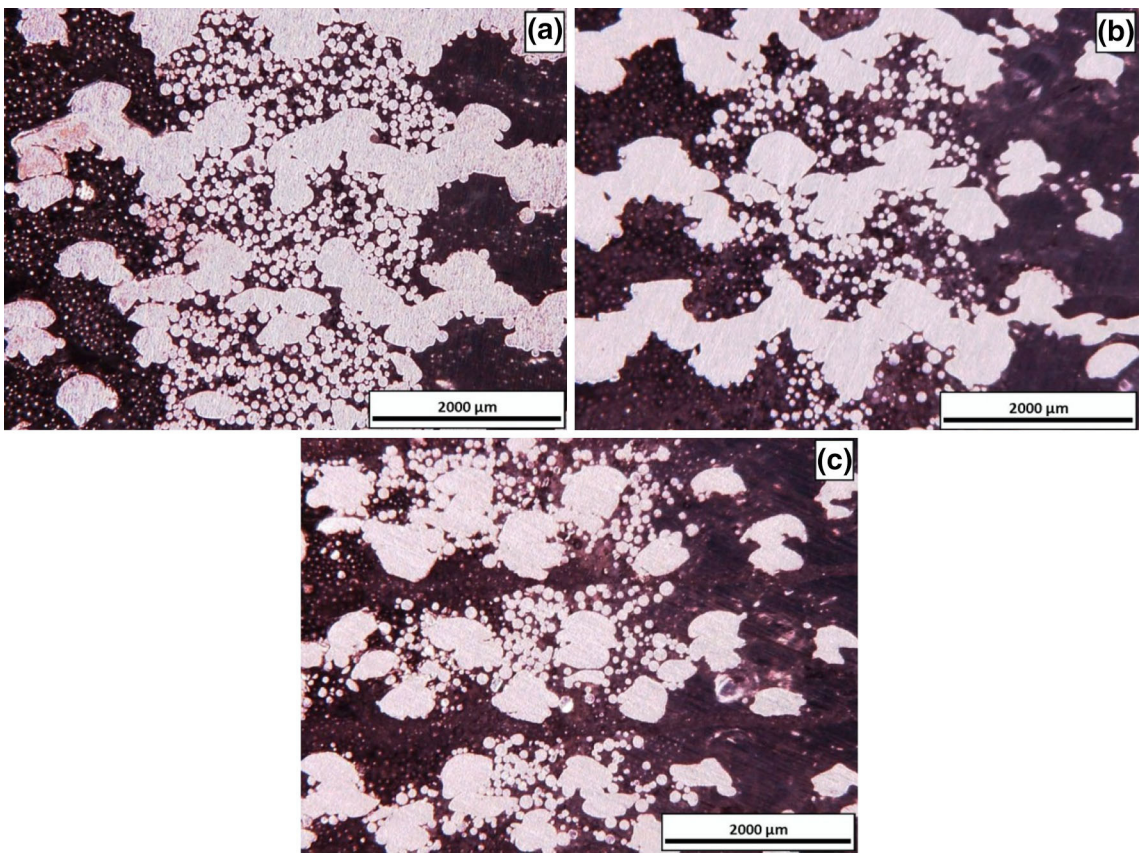

Fig. 8. Microscopic observations from the cross section of (a) unetched, (b) 90 s etched, and (c) 120 s etched hexagonal cubes with Hirox KH-7700 digital microscope under ×50 magnification.

Journal : 11837_JOM Dispatch : 31-1-2015 Pages : 8
Article No.: 1307 ☐ LE ☑ CP ☐ TYPESET ☑ DISK

powder, the "frame" only extends for about 2 mm into the structure, resulting in a lower density of powder in the center of the part. During the etching cycle, the looser powder in the center portion is removed faster while the "frame" of denser powder stays more intact. The micrographs in Fig. 8 show that even the compacted powder is being removed by the etching but at a much slower rate. If the etching were to be continued until the denser "frame" was completely cleared, then the integrity of the structure would most likely be lost. Other approaches to remove trapped powder within the lattice structures should be explored. Suggested methods are ultrasonic bath and mechanical vibrations via a vibrating plate. Another approach is to directly etch the specimens without blasting them first.

ACKNOWLEDGMENTS

This research was supported by the Fitts Department of Industrial and Systems Engineering and the Laboratory for Additive Manufacturing and Logistics at North Caroline State University.

REFERENCES

1. J. Banhart, *Prog. Mater Sci.* 46, 559 (2001).
2. O.L.A. Harrysson, O. Cansizoglu, D.J. Marcellin-Little, D.R. Cormier, and H.A. West II, *Mater. Sci. Eng. C* 28, 366 (2008).
3. C.K. Chua, K.F. Leong, C.M. Cheah, and S.W. Chua, *Int. J. Adv. Manuf. Technol.* 21, 291 (2003).
4. X. Li, C. Wang, W. Zhang, and Y. Li, *Rapid Prototype J.* 16, 44 (2010).
5. O. Cansizoglu (Ph.D. dissertation, North Carolina State University, 2008).
6. L.J. Gibson and M.F. Ashby, *Cellular Solids: Structure & Properties*, 2nd ed. (Cambridge, U.K.: Cambridge University Press, 1997).
7. M.F. Ashby, *Philos. Trans. R. Soc. A* 364, 15 (2006).
8. H.N.G. Wadley, *Philos. Trans. R. Soc. A* 364, 31 (2006).
9. G.F. Vander Voort, *Metallography Principles and Practice* (Materials Park, OH: ASM International, 1999).
10. C.S. Wen and Y.T. Yu, *Surf. Coat. Technol.* 176, 337 (2004).
11. D. Brunette, P. Tengvall, M. Textor, and P. Thomsen, *Titanium in Medicine: Material Science, Surface Science, Engineering, Biological Response and Medical Applications* (Berlin, Germany: Springer, 2001).

Journal : 11837_JOM | Dispatch : 31-1-2015 | Pages : 8
Article No.: 1307 | ☐ LE ☑ CP | ☐ TYPESET ☑ DISK

Journal : **11837**
Article : **1307**

Springer
the language of science

Author Query Form

Please ensure you fill out your response to the queries raised below and return this form along with your corrections

Dear Author

During the process of typesetting your article, the following queries have arisen. Please check your typeset proof carefully against the queries listed below and mark the necessary changes either directly on the proof/online grid or in the 'Author's response' area provided below

Query	Details Required	Author's Response
AQ1	Please confirm the inserted city name in Affiliation 1 is correct and amend if necessary.	